

Published in final edited form as:

Lab Invest. 2017 August ; 97(8): 983–991. doi:10.1038/labinvest.2017.49.

Microfluidics for rapid cytokeratin immunohistochemical staining in frozen sections

Saska Brajkovic^{1,2}, Diego G. Dupouy^{1,2}, Laurence de Leval³, and Martin A. M. Gijs^{1,*}

¹Laboratory of Microsystems, Ecole Polytechnique Fédérale de Lausanne, CH-1015, Switzerland

²Lunaphore Technologies SA, EPFL Innovation Park - Building C, CH-1015, Lausanne, Switzerland ³Institute of Pathology, Centre Hospitalier Universitaire Vaudois and University of Lausanne, CH-1011 Lausanne, Switzerland

Abstract

Frozen sections (FS) of tumor samples represent a cornerstone of pathological intraoperative consultation and play an important role in the microscopic analysis of specimens during surgery. So far, immunohistochemical (IHC) stainings on FS have been demonstrated for a few markers using manual methods. Microfluidic technologies have proven to bring substantial improvement in many fields of diagnostics, though only a few microfluidic devices have been designed to improve the performance of IHC assays. In this work, we show optimization of a complete pan-cytokeratin chromogenic immunostaining protocol on FS using a microfluidic tissue processor, into a protocol taking less than 12 minutes. Our results showed specificity and low levels of background. The dimensions of the microfluidic prototype device are compatible with the space constraints of an intraoperative pathology laboratory. We therefore anticipate that the adoption of microfluidic technologies in the field of surgical pathology can significantly improve the way FSs influence surgical procedures.

Introduction

Frozen sections (FS) play an important role in the microscopic analysis of specimens during surgery. Surgeons may require an intraoperative consultation from pathologists for different purposes, ranging from the assessment of a resection margin in a tissue-conserving procedure, to the determination of a metastatic condition or the identification of the possible nature of lesions in exploratory surgeries¹. In a large number of FS consultations, hematoxylin and eosin staining (H&E) is used by pathologists to seek whether the tumoral dissection presents a clear margin. Although the cost-benefit of the exhaustive use of FS is

Users may view, print, copy, and download text and data-mine the content in such documents, for the purposes of academic research, subject always to the full Conditions of use:http://www.nature.com/authors/editorial_policies/license.html#terms

*Correspondence to: martin.gijs@epfl.ch, TE: +41 21 69 36734.

Disclosure: D.G.D. and S.B., at the submission of the paper, are partially employed at Lunaphore Technologies SA, which is commercializing the MTP-based technology. D.G.D and M.A.M.G. have equity interest in Lunaphore Technologies SA.

Author Contributions: S.B., D.G.D., L.d.L. and M.A.M.G. designed the study; S.B. ran the experiments and image acquisition; S.B., D.G.D., L.d.L. and M.A.M.G. analyzed the results; D.G.D. designed the figures; D.G.D., S.B. and M.A.M.G wrote the paper; all authors reviewed it.

under discussion for some procedures^{2,3}, the clinical advantage is clear in most cases. Even for breast carcinomas, where cryosectioning is troublesome due to the high fat content⁴, studies showed that intraoperative assessment via gross examination and H&E of the margins can significantly decrease the re-operative rates^{5,6}. Intraoperative methods based on H&E alone, even though very specific, often lack sensitivity⁷, which can be attributed to the absence of cancer cell-specific staining. Under these conditions, interpretation mostly relies on the experience of the pathologist, and a small number of infiltrating cancer cells into healthy tissue may not be easily recognizable. Studies show that false negative cases can reach values of 50% when the tumor size is smaller than 2 mm in breast cancer surgery, and that this rate can be significantly reduced using cytokeratin (CK) staining for intraoperative consultation of sentinel lymph nodes³. Numerous additional immunohistochemical markers would be interesting to test during intraoperative consultations, if only the turn-around time was not a limitation. Only for a few particular intraoperative consultations, immunohistochemistry (IHC) tests are available today. An example is the rapid IHC test for sentinel lymph nodes, which helps pathologists assess whether the lesions have metastasized and surgeons determine what is the extent of the dissection.^{7–11} Another example is Mohs surgery of melanomas, where real-time margin analysis is required in order to ensure the lesion was fully dissected, while a maximum tissue preservation is guaranteed. IHC techniques using anti melanoma antigen recognized by T cell 1 (MART-1) antibodies have been proposed.^{12–14} A rapid (10 min) IHC test for the proliferation marker Ki-67 was also proposed as an adjunct to morphological diagnosis and grading of astrocytic tumors that can be performed intraoperatively.¹⁵ All these methods were based on the use of rapid IHC kits, specifically developed for a particular marker and tissue type, hindering more general use of the technique on other specimens and/or other markers of interest.

Technological improvements have significantly increased the throughput of IHC assays on formalin-fixed paraffin-embedded (FFPE) samples run by automated machines, both by reducing the staining time and parallelizing the number of assays. The first automats mimicked manual stainings by dropping reagents on top of horizontally disposed slides¹⁶. Nowadays, Ventana Medical Systems makes use of an inert liquid to avoid evaporation, and airstreams to increase reagent mixing¹⁶. The latest technology from Dako uses capillary forces to drive reagents by opening and closing the gap between the slide and a movable coverslip, and claims a turn-around time of 2.5 h for IHC^{16,17}, showing the importance of boosting the reagent transport over the tissue section. Increased reagent transport has also been achieved in research settings by making use of an alternating electrical field on top of the tissue, leading to faster IHC staining^{18,19}. We have recently demonstrated that the use of microfluidics allowed to achieve fast immunostaining (<10 min) on FFPE sections with reagents that would normally require a minimum of 2 hours upon manual or automat-based process.^{20,21} So far, the capabilities of this technology have only been demonstrated for immunofluorescence staining of human epidermal growth factor receptor 2 (HER2) and CK.

In this work, we developed a complete pan-CK chromogenic staining protocol on FS using a microfluidic tissue processor (MTP) as the core technology of our stainer. Starting from an existing 43-min microfluidic protocol set up in our laboratory, we optimized each step to a working protocol in less than 20 min, including tissue preparation after cryosectioning in 7 minutes and immunohistochemical staining in less than 12 minutes. This optimized

protocol was tested on different frozen tissue types. Since the increased time performance relies on the microfluidic handling and not on the reagents themselves, our technique has the potential to provide pathologists with a versatile tool for fast IHC stainings on frozen sections of any type. Moreover, the microfluidic characteristics allowed us to develop an experimental prototype that matches the space constraints often found in FS laboratories. We believe that many more questions could be answered intraoperatively with the use of our new technology to reduce the turn-around time of IHC assays.

Material and Methods

Sample preparation

Anonymized frozen samples were obtained from the Institute of Pathology at the Centre Hospitalier Universitaire Vaudois (CHUV). Ethical approval was obtained from the “Commission cantonale d'éthique de la recherche sur l'être humain” (CER-VD) under the protocol number 511/12. The samples included ureter, pancreas, prostate, breast carcinoma, pancreas adenocarcinoma, lung adenocarcinoma (NSCLC) and Hodgkin lymphoma. The details of the protocol steps are shown in Table 1. Frozen tissue blocks were cut with a cryostat (Leica, CM1850) with a thickness of 4 and 10 microns, and mounted on standard histopathology slides (step 1) at the Histology Core Facility (HCF) of the Ecole Polytechnique Fédérale de Lausanne (EPFL). In the optimized MTP protocol (Table 1iii), sections were dried (step 2) using cold air of an air-flow dryer for 2 min, fixed (step 3) for 3 min in cold acetone (kept at -20°C prior to the experiment, Fischer Chemicals, A/0600/15) and dried again (step 4) with the air-flow dryer using cold air for 2 min. All the subsequent steps of the staining were performed on the MTP-device (referred to as “On chip” in Table 1). Several reagents were tested during optimization of the pre-staining steps: fixation with methanol during 10 min (-20°C, Fischer Chemicals, M/4000/15) immediately after sectioning; fixation with acetone for 10 min (on ice, Fischer Chemicals, A/0600/15) immediately after sectioning; and tissue dehydration at temperature for 15 min or using air flow for 2 min.

Microfluidic setup

Once the frozen sample preparation is completed, the tissue section is clamped using a gasket to the MTP to form a reaction chamber of 17x17 mm², after which the system is ready for fast IHC staining (Figure 1a). Reagents are delivered through microfluidic channels in the chip to the reaction chamber, where the staining takes place (Figure 1b). The MTP enables a fast fluidic exchange on a one-second timescale. Additional details about the MTP working principle can be found elsewhere²⁰. Figure 1c shows a schematic of the automated pressure-driven laboratory setup that was used for the experiments. The setup consisted of: (i) 50 mL reservoirs used for common reagents, namely phosphate-buffered saline (PBS), deionized water (DIW), 3,3'-diaminobenzidine (DAB), and ethanol; (ii) 1.5 mL Eppendorf tubes for specific reagents, such as antibodies, blocking solutions and hematoxylin; (iii) a computer-operated valve-manifold called Reagent Delivery System (RDS) used to select among the reagents to be flushed into the reaction chamber; (iv) the MTP/tissue sample staining chamber. Figure 1d shows a picture of the prototype used for the

experiment. The inset (i) shows the manual mechanism for insertion of the MTP in the machine.

MTP-based stainings

After the tissue was dried and clamped to the MTP, the “On chip” steps in columns (ii) and (iii) from Table 1 were performed. The protocol was defined on a graphical user interface and executed entirely by the automated laboratory setup. Tissue rehydration (step 5) and all the washing steps were realized using Tris Buffered Saline solution (TBS, Sigma Life Science, T5912-1L). Blocking solutions (step 6 and 7) were not used in the optimized MTP protocol. Primary antibody (Ab) incubation (step 8) was done using mouse anti-human CK (Dako, M3515), diluted 1/100 in TBS Tween 0.05% (Tween 20, Fischer Scientific, BP337-100). The step of incubation with post-primary Ab (step 9) used in column (ii) was not performed in the optimized protocol of column (iii). After primary Ab application, tissue sections were directly incubated with ImmPRESS (Vector Laboratories, MP-7402), a micro-polymer conjugated with anti-mouse secondary Ab and horseradish peroxidase (HRP) enzyme molecules (step 10). The reaction was revealed (step 11) using the 3,3'-diaminobenzidine (DAB) chromogen (ImmPACT, Vector SK-4105) and the nuclei counterstaining (step 12) was achieved using hematoxylin Gill3 20% (Thermo Scientific, 72604). Finally, slides were washed, unclamped from the MTP and coverslipped (mounting solution from Sigma, F6182-20). All negative controls (CTL) were obtained by performing a parallel staining by replacing the primary Ab by a solution of TBS Tween 0.05%.

During optimization, alternative detection kits were tested: ImmPRESS Excel (Vector, MP-7602), Novolink (Novocastra, Biosystems, RE7290), and Quanto (Thermo Scientific, TL-060-QHD). Each of these kits provided its own peroxidase block (step 6), protein block (step 7), amplifier or post-primary Ab (step 9), polymer (step 10) and DAB buffer (step 11). Additional DAB chromogens were tested: DAB EqV (Vector, MP-7602), DAB Reveal (Spring, DABC-001/15), DAB Novolink (Novocastra, Biosystems, RE7105/06), DAB Metal enhanced (Thermo Scientific 34065/1855910). Counterstaining tests were also done with hematoxylin from Novolink (Novocastra, Biosystems, RE7107) and hematoxylin QS (Vector H-34004).

H&E stainings

The total time needed for the optimized H&E protocol execution was 2:30 min. Slides were stained with hematoxylin QS (Vector, H-34004) and then rinsed with tap water. A second rinsing was then applied using ethanol 100% (Fischer Chemical, E/0650DF/15). Subsequently, tissue sections were stained using eosin Y 1% (Sigma, E4382) in 70% ethanol with 1% phloxine (Fluka, 28550) for 15 s, rinsed again with ethanol 100% and then tap water. Finally, specimens were unclamped from the MTP and coverslipped using DPX mounting media for histology (Sigma, 06522-100ML).

Imaging

Images of stained slides were taken using a slide scanner (VS-ASW FL, Olympus) with a 20x 0.75 NA objective. A color depth of 24-bit and a resolution of 346 nm/pixel was

achieved and saved in .vsi format. The extracted images were exported as TIFF images using Fiji Image J and a plugin provided by the Bioimaging and Optics Platform (BIOP) of EPFL.

Manual controls

Manual staining controls were performed using the exact same dilutions and incubation times as in the optimized MTP-based stainings and are detailed in column (iii) of Table 1. Due to the need of manually handling the tissue, an additional 5 minutes per slide were required to remove the excess of liquid in between incubation steps.

Results

Pre-staining protocol optimization

The common tissue preparation steps, referred to as “pre-staining” in Table 1, were optimized on ureter autopsy specimens, from an initial total time of 55 min to a final time of 8 min. The five pre-staining steps were (1) sectioning, (2) first drying, (3) fixation, (4) second drying, and (5) re-hydration. Step 1 was not optimized, as being part of a service from HCF. Steps 2 to 4 were optimized off-chip, while step 5 was first performed off-chip (column (ii) of Table 1), then included on-chip (column (iii) of Table 1). Figure 2a shows a comparison of CK staining obtained using fixation by methanol (at 4°C) and acetone (kept at -20°C prior to the experiment). In direct acetone fixation, the tissue is immersed in acetone immediately after sectioning, while for the indirect mode, the tissue is sectioned, dried for 15 min at room temperature, and then immersed in acetone. Indirect fixation with acetone showed the best staining. In Figure 2b, the optimization of the acetone indirect fixation time is shown, where fixation times between 10 min to 1 min were tested. Three-minute fixation turned out to be sufficient to obtain a clear staining. Increasing the fixation time above three minutes resulted in no apparent improvement, while shorter fixation times increased the areas where the staining was not present or was fainter. Figure 2c depicts the results of the optimization of the second drying time (step 4 in Table 1), showing satisfactory results using cold air of an air-flow dryer for 2 min, instead of passive drying over 15 min. The same drying procedure was applied for first drying in step 2. Figure 2d shows how the rehydration step, prior to staining, could be successfully achieved in 1 min, once the slide was clamped to the MTP.

MTP staining protocol staining protocol optimization

Once the optimum times for the pre-staining steps were found, the choice of ImmPRESS as our detection system was done based on a direct comparison test that can be found in the Supplementary Information (Figure S1). Subsequently, the steps corresponding to “staining part I” of Table 1 were optimized. Figure 3a shows that the use of a blocking buffer, standardly done in the manual protocol, did not improve the quality of the staining in microfluidic IHC, which was the reason why it was removed from the optimized protocol in column (iii) of Table 1. Figure 3b and 3c show the optimization of the primary Ab and the secondary Ab incubation times, respectively. Incubation during 2 min for the primary Ab and 4 min for the secondary Ab were sufficient to obtain a high-quality staining. Such short Ab incubation times using the MTP technology had already been demonstrated before for immunohistofluorescence assays in our laboratory^{20,21}.

“Staining part II” steps from Table 1 were optimized by both the choice of the reagents that gave the best imaging result and the shortest incubation times. Figure 4a shows the incubation time optimization of the DAB obtained from the kit Novolink, which was used as our reference standard during the experiments described above. Increasing the DAB incubation time between 30 s and 90 s showed an increment in the intensity of staining. However, no difference was perceived between 90 s and 150 s, indicating that incubation longer than 90 s was not necessary. Subsequently, DAB reagents from five different providers were compared under the same experimental conditions and shown in Figure 4b. ImmPACT was selected as giving the best staining results in the IHC MTP settings. Similarly, in Figure 4c, three hematoxylin suppliers were compared, giving Gill3 as the most suitable choice of hematoxylin for our experiments. The incubation time of Gill 3 hematoxylin was optimized down to 15 s (Figure 4d). Finally, the hematoxylin solution was diluted to 20% of its original concentration using DIW, resulting in lesser viscosity without compromising staining (Figure 4e).

Optimized MTP H&E and CK staining results for different tissue types

Figure 5 shows images of the H&E (first column), CTL (negative control, second column) and CK (third column) stains using the MTP optimized protocols, performed on the following samples: pancreas, ureter, prostate, breast carcinoma, pancreas adenocarcinoma, lung carcinoma (NSCLC) and Hodgkin lymphoma. Successful H&E stains were achieved for all the tissue types used in our study and the turn-around time was 2 minutes and 30 seconds. CK staining showed specificity to epithelial cells on non-cancerous tissues and on carcinomas of different origin. At the same time, no false-positive staining was observed on lymphoma cases. Similarly, the negative controls, where the protocols were run without primary anti-CK Abs, showed only nuclear counterstaining, as expected.

Manual controls

Manual staining experiments were performed on all the tissues shown in Figure 5 using the incubation times of the on-chip experiments, as detailed in Table 1 (iii). The images of these stainings are shown in Figure S2 of the supplementary information. Results showed that in most cases the background is significantly higher when compared to on-chip experiments.

Discussion

Microfluidics has already proven to bring substantial improvement in many fields of diagnostics, with point-of-care applications being the most popular²². Seemingly, laboratory-based microfluidics enabled improvements in genomics, sequencing, high-throughput screening, and separations. The higher surface-to-volume ratio achieved by handling reagents in the micrometer scale allows for higher sensitivity and assay turn-around-time. Surprisingly enough, only a few microfluidic devices have been designed to improve the performance of IHC assays used in the field of tissue diagnostics^{23,24}. While these devices confine the staining on a small portion of the tissue section, the MTP is designed to deliver and wash reagents over the entire tissue surface in down to one second.

We demonstrated that our microfluidic technology can deliver fast (<12 min) and automated IHC stains using conventional anti-CK Abs on multiple frozen tissue types. Results showed specificity to cells of epithelial origin and low levels of background in the negative controls. The dimensions of the prototype used for the experiments is compatible with the space constraints typically observed in intraoperative laboratories. The need for fast pathological examination during surgery makes FSs one of the most challenging tasks that the pathologist performs in practice. As of today, except for a few dedicated fast IHC kits^{7–15,18,25}, intraoperative diagnosis is based on H&E alone and confronted post-operatively to the corresponding permanent sections. Rapid and automated IHC tests made available at the intraoperative laboratory would significantly add to the accuracy of the diagnosis for the most complicated cases. The method developed in this study is limited to only one marker. Reproducibility was addressed using the same protocol for 7 different tissue types, which is not sufficient for a full validation of the protocol. Cases were selected retrospectively and frozen samples were cut on demand, thus neither represents a validation for a clinical use nor for any specific use of the marker. A prospective study is required to attribute clinical value. Finally, even though this method performed well on tissue sections where the marker of interest is highly expressed, there is no evidence that it will reach the level of sensitivity required for some assays. Analytical sensitivity and specificity was not addressed quantitatively in this study. It is clear that more is to be done in order to offer pathologists a tool for IHC diagnosis on FSs, in particular the availability of a broader panel of markers. We anticipate that the adoption of microfluidic technologies in the field of surgical pathology can then significantly improve the way FS analysis influence surgical procedures.

Supplementary Material

Refer to Web version on PubMed Central for supplementary material.

Acknowledgments

We acknowledge the Histology department of EPFL, in particular Jessica Dessimoz and Gianni Mancini for performing the sectioning of frozen blocks on-demand, enabling the performance of an intraoperative-like FS staining.

Funding: This work was funded by the Proof-of-Concept ERC grant 662449 - IntraMEMS ERC-2014-PoC. D.G.D is partially supported by the National Competence Center for Biomedical Imaging (NCCBI.ch).

References and Notes

1. Lechago J. The Frozen Section: Pathology in the Trenches. *Arch Pathol Lab Med.* 2005; 129:1529–1531. [PubMed: 16329724]
2. Osborn JB, Keeney GL, Jakub JW, Degen AC, Boughey JC. Cost-Effectiveness Analysis of Routine Frozen-Section Analysis of Breast Margins Compared with Reoperation for Positive Margins. *Ann Surg Oncol.* 2011; 18:3204–3209. [PubMed: 21861234]
3. Holm M, et al. Intraoperative immunohistochemistry staining of sentinel nodes in breast cancer: Clinical and economical implications. *The Breast.* 2008; 17:372–375. [PubMed: 18490162]
4. Emmadi R, Wiley EL. Evaluation of Resection Margins in Breast Conservation Therapy: The Pathology Perspective—Past, Present, and Future. *Int J Surg Oncol.* 2012; 2012:1–9.
5. Jorns JM, et al. Intraoperative Frozen Section Analysis of Margins in Breast Conserving Surgery Significantly Decreases Reoperative Rates: One-Year Experience at an Ambulatory Surgical Center. *Am J Clin Pathol.* 2012; 138:657–669. [PubMed: 23086766]

6. Boughey JC, et al. Impact of analysis of frozen-section margin on reoperation rates in women undergoing lumpectomy for breast cancer: Evaluation of the National Surgical Quality Improvement Program data. *Surgery*. 2014; 156:190–197. [PubMed: 24929768]
7. Stovgaard ES, Tvedskov TF, Lænkholm AV, Balslev E. Cytokeratin on Frozen Sections of Sentinel Node May Spare Breast Cancer Patients Secondary Axillary Surgery. *Pathol Res Int*. 2012; 2012:1–5.
8. Nahrig JM, et al. Intraoperative Examination of Sentinel Lymph Nodes by Ultrarapid Immunohistochemistry. *Breast J*. 2003; 9:277–281. [PubMed: 12846860]
9. Leikola JP, Toivonen TS, Krogerus LA, von Smitten KAJ, Leidenius MHK. Rapid immunohistochemistry enhances the intraoperative diagnosis of sentinel lymph node metastases in invasive lobular breast carcinoma. *Cancer*. 2005; 104:14–19. [PubMed: 15929120]
10. Johnston EI, Beach RA, Waldrop SM, Lawson D, Cohen C. Rapid Intraoperative Immunohistochemical Evaluation of Sentinel Lymph Nodes for Metastatic Breast Carcinoma. *Appl Immunohistochem Mol Morphol*. 2006; 14:57–62. [PubMed: 16540732]
11. Lee I-K, et al. Intraoperative examination of sentinel lymph nodes by immunohistochemical staining in patients with breast cancer. *Eur J Surg Oncol EJSO*. 2006; 32:405–409. [PubMed: 16524688]
12. Bricca GM, Brodland DG, Zitelli JA. Immunostaining Melanoma Frozen Sections: The 1-Hour Protocol. *Dermatol Surg*. 2004; 30:403–408. [PubMed: 15008870]
13. Kimyai-Asadi A, Ayala GB, Goldberg LH, Vujevich J, Jih MH. The 20-Minute Rapid MART-1 Immunostain for Malignant Melanoma Frozen Sections. *Dermatol Surg*. 2008; 34:498–500. [PubMed: 18248466]
14. Chang KH, et al. Novel 16-minute technique for evaluating melanoma resection margins during Mohs surgery. *J Am Acad Dermatol*. 2011; 64:107–112. [PubMed: 21167405]
15. Haapasalo J. Ultrarapid Ki-67 immunostaining in frozen section interpretation of gliomas. *J Clin Pathol*. 2005; 58:263–268. [PubMed: 15735157]
16. Rasmussen, OF., Binzer, T., Rudbeck, L. Dynamic Gap Staining A New IHC Staining Technology. Dako: 2014.
17. Dako Denmark A/S. [accessed 22.08.16] Dako Omnis Data Sheet. http://www.dako.com/ch/29067_dako-omnis-data-sheet.pdf
18. Toda H, et al. A Novel Immunohistochemical Staining Method Allows Ultrarapid Detection of Lymph Node Micrometastases While Conserving Antibody. *ACTA Histochem Cytochem*. 2011; 44:133–139. [PubMed: 21753859]
19. R-IHC Study Group. et al. Rapid immunohistochemistry based on alternating current electric field for intraoperative diagnosis of brain tumors. *Brain Tumor Pathol*. 2015; 32:12–19. [PubMed: 24807101]
20. Ciftlik AT, Lehr H-A, Gijs MAM. Microfluidic processor allows rapid HER2 immunohistochemistry of breast carcinomas and significantly reduces ambiguous (2+) read-outs. *Proc Natl Acad Sci*. 2013; 110:5363–5368. [PubMed: 23479638]
21. Dupouy DG, et al. Continuous quantification of HER2 expression by microfluidic precision immunofluorescence estimates HER2 gene amplification in breast cancer. *Sci Rep*. 2016; 6:20277. [PubMed: 26856369]
22. Chin CD, Linder V, Sia SK. Commercialization of microfluidic point-of-care diagnostic devices. *Lab Chip*. 2012; 12:2118. [PubMed: 22344520]
23. Kim MS, et al. Breast Cancer Diagnosis Using a Microfluidic Multiplexed Immunohistochemistry Platform. *PLoS ONE*. 2010; 5:e10441. [PubMed: 20454672]
24. Lovchik RD, Kaigala GV, Georgiadis M, Delamarche E. Micro-immunohistochemistry using a microfluidic probe. *Lab Chip*. 2012; 12:1040. [PubMed: 22237742]
25. Glass LF, et al. Rapid Frozen Section Immunostaining of Melanocytes by Microphthalmia-Associated Transcription Factor. *Am J Dermatopathol*. 2010; :1.doi: 10.1097/DAD.0b013e3181bcd94f [PubMed: 20098079]

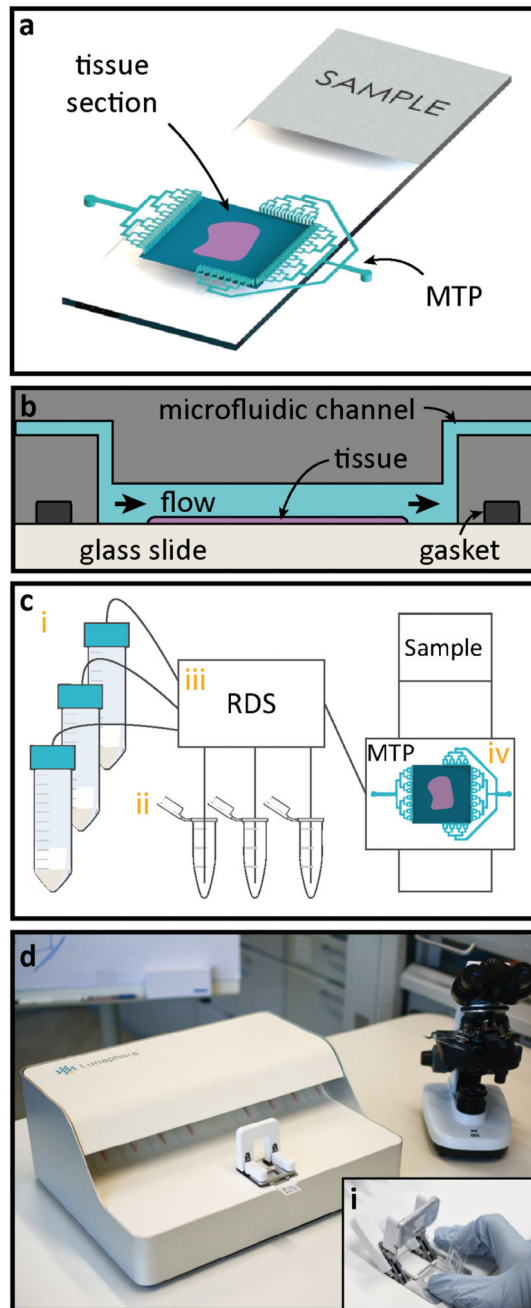


Fig. 1. Working principle of microfluidic staining of FS.

(a) Once the frozen sample preparation is completed, the sample is clamped using a gasket to the Microfluidic Tissue Processor (MTP) to form a reaction chamber of $17 \times 17 \text{ mm}^2$, after which the system is ready for fast IHC staining. Microfluidic channels deliver reagents to and from the reaction chamber. Staining takes place only in the chamber (b) Schematic cross-section of the MTP clamped to the tissue slide. Inside the reaction chamber, reagents are sequentially delivered and washed over the surface of the tissue section. The MTP enables a fast fluidic exchange on a one-second timescale, while keeping reagent exposure

times uniform throughout the whole tissue surface. (c) Schematics of the laboratory setup used for the experiments: (i) 50 mL reservoirs are used for common reagents, namely PBS, DIW, DAB, and hematoxylin; (ii) 1.5 mL Eppendorf tubes are used to load specific reagents, such as antibodies, and blocking solutions; (iii) a computer-operated valve-manifold called Reagent Delivery System (RDS) allows for the selection of the reagents that are flushed into the chamber of reaction; (iv) MTP/ tissue sample staining chamber. (d) Picture of the prototype used for the experiments. The inset (i) shows the mechanism of manual insertion of the MTP in the machine.

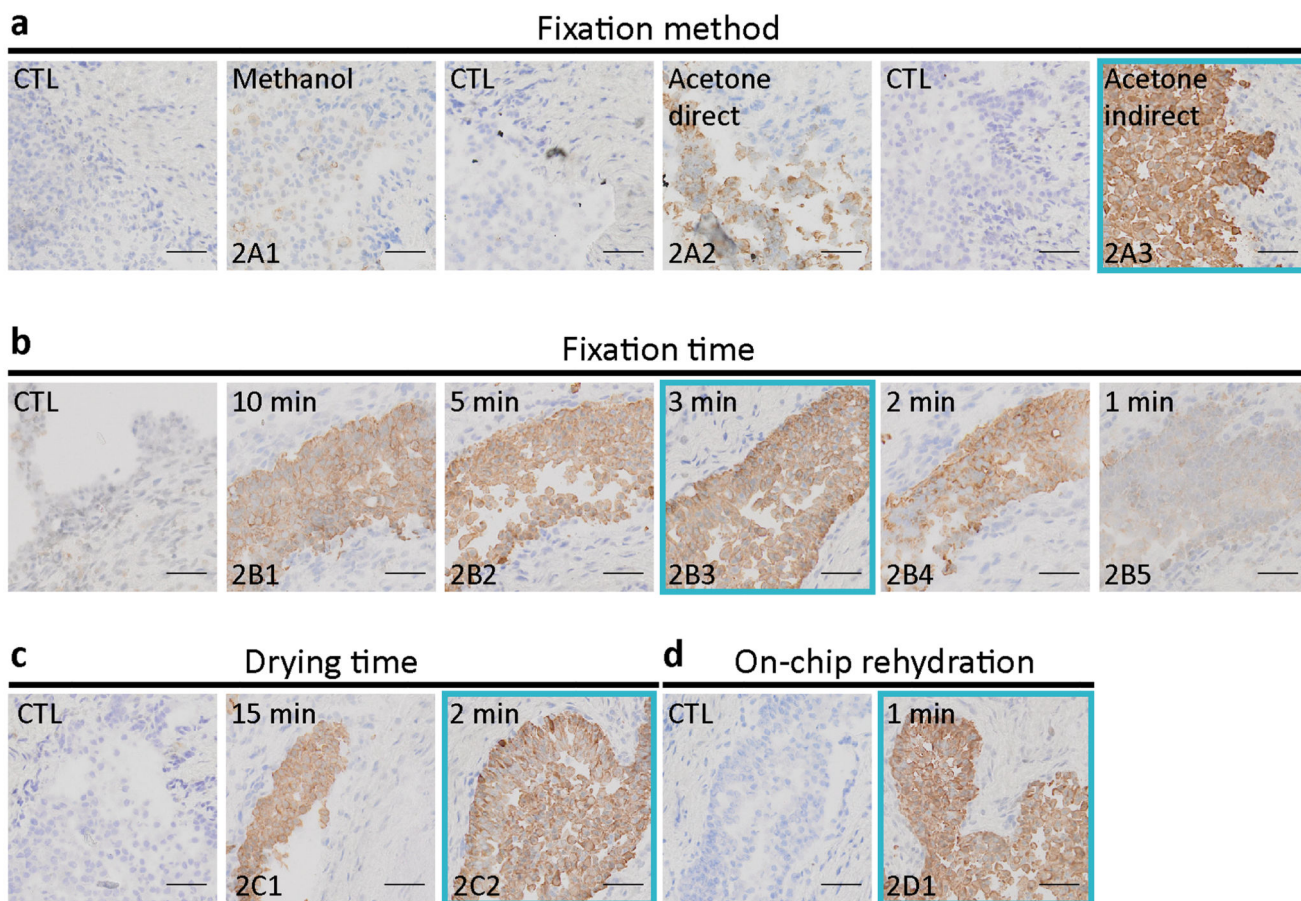


Fig. 2. Optimization of the pre-staining protocol on ureteral biopsy sections.

Slides show the final CK staining and are compared with negative control (CTL) samples, obtained by staining without use of the primary Ab, in which case, ideally, only nuclear hematoxylin counterstaining is visible. The immunohistochemical staining of frozen sections described in this work requires a set of common tissue preparation steps (see Table 1): (1) sectioning, (2) first drying, (3) fixation, (4) second drying, and (5) re-hydration. Step 1 was neither optimized nor counted within the total time of the IHC assay. Steps 2 to 4 were optimized off-chip. **(a)** Comparison of CK staining obtained using fixation by methanol (at 4°C) and acetone (kept at -20°C prior to the experiment). In direct acetone fixation, the tissue is immersed in the acetone immediately after sectioning. Indirect means that the tissue is sectioned, dried for 15 min at room temperature, and then immersed in the acetone. Indirect fixation with acetone showed best staining. **(b)** Optimization of the acetone indirect fixation time. Three-minute fixation turned out to be sufficient to obtain a clear staining. Increasing the fixation time resulted in no apparent improvement, while shorter fixation times increased the areas where the staining was not present or was fainter. **(c)** Optimization of the second drying time (step 4 in Table 1) showed satisfactory results using an air-flow dryer for 2 min. **(d)** One-minute successful re-hydration was achieved by clamping the section to the MTP. The blue frames on each panel represent the ‘best conditions’ chosen for

the final experiments of Figure 5 and are represented in column (iii) of Table 1 (Scale bars: 50 μm ; bottom-left code: identifier of the sample in Table S1).

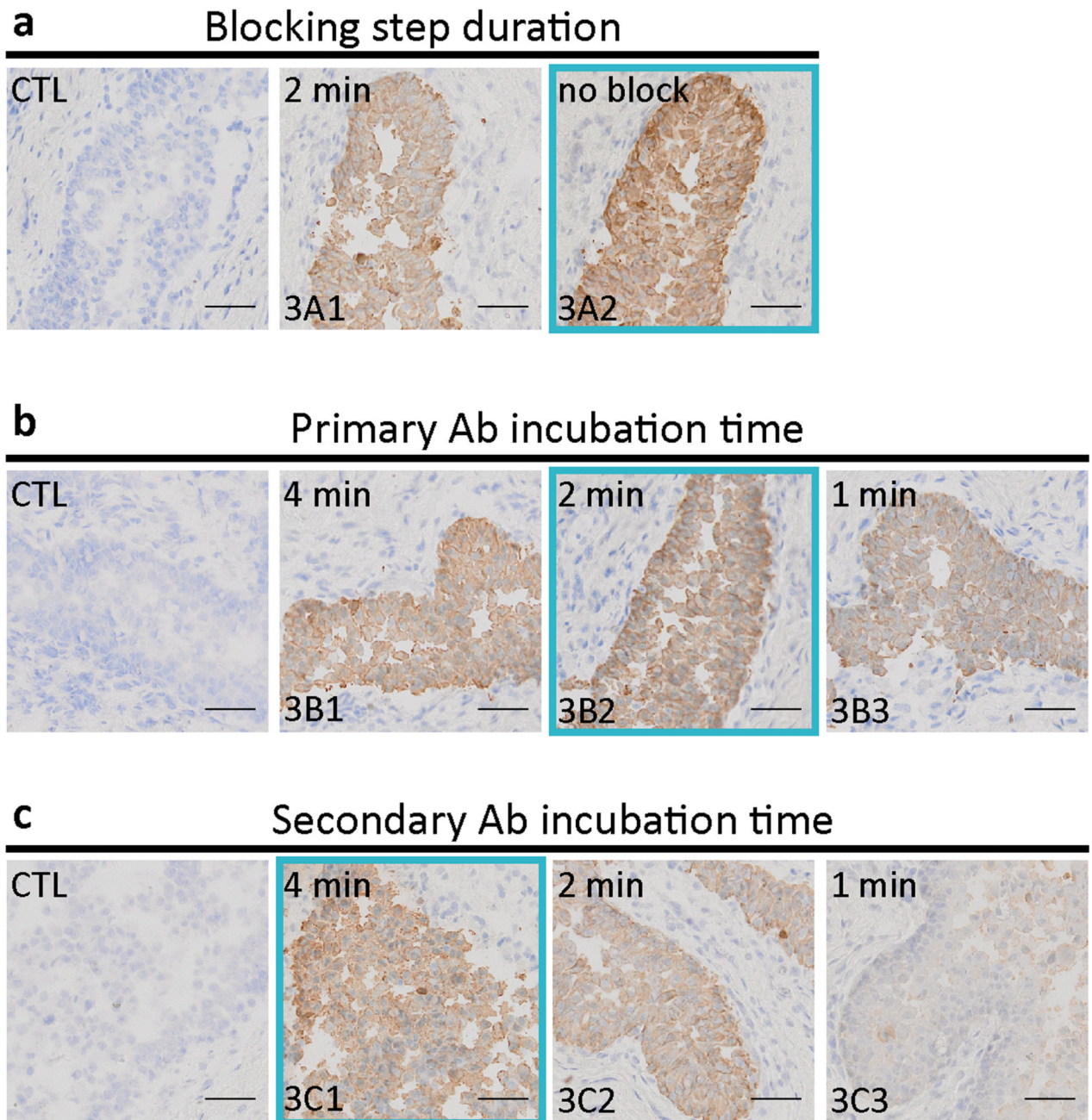


Fig. 3. Optimization of the first part of the MTP staining protocol of Table 1 on ureteral biopsy sections.

Slides show the final CK staining and are compared with CTL samples, obtained by staining without use of the primary Ab. (a) Use of a blocking buffer, standardly done in the manual protocol, did not improve staining in microfluidic IHC, which was the reason to remove the blocking step from the optimized protocol in column (iii) of Table 1. (b) Optimization of the primary Ab incubation time. Incubation during 2 min was sufficient to obtain a high-quality staining. (c) Optimization of the secondary Ab incubation time. 4 min was chosen in the

initial MTP protocol of column (ii) of Table 1. The blue frames on each panel represent the 'best conditions' chosen for the final experiments of Figure 5 and are represented in column (iii) of Table 1. (Scale bars: 50 μm ; bottom-left code: identifier of the sample in Table S1).

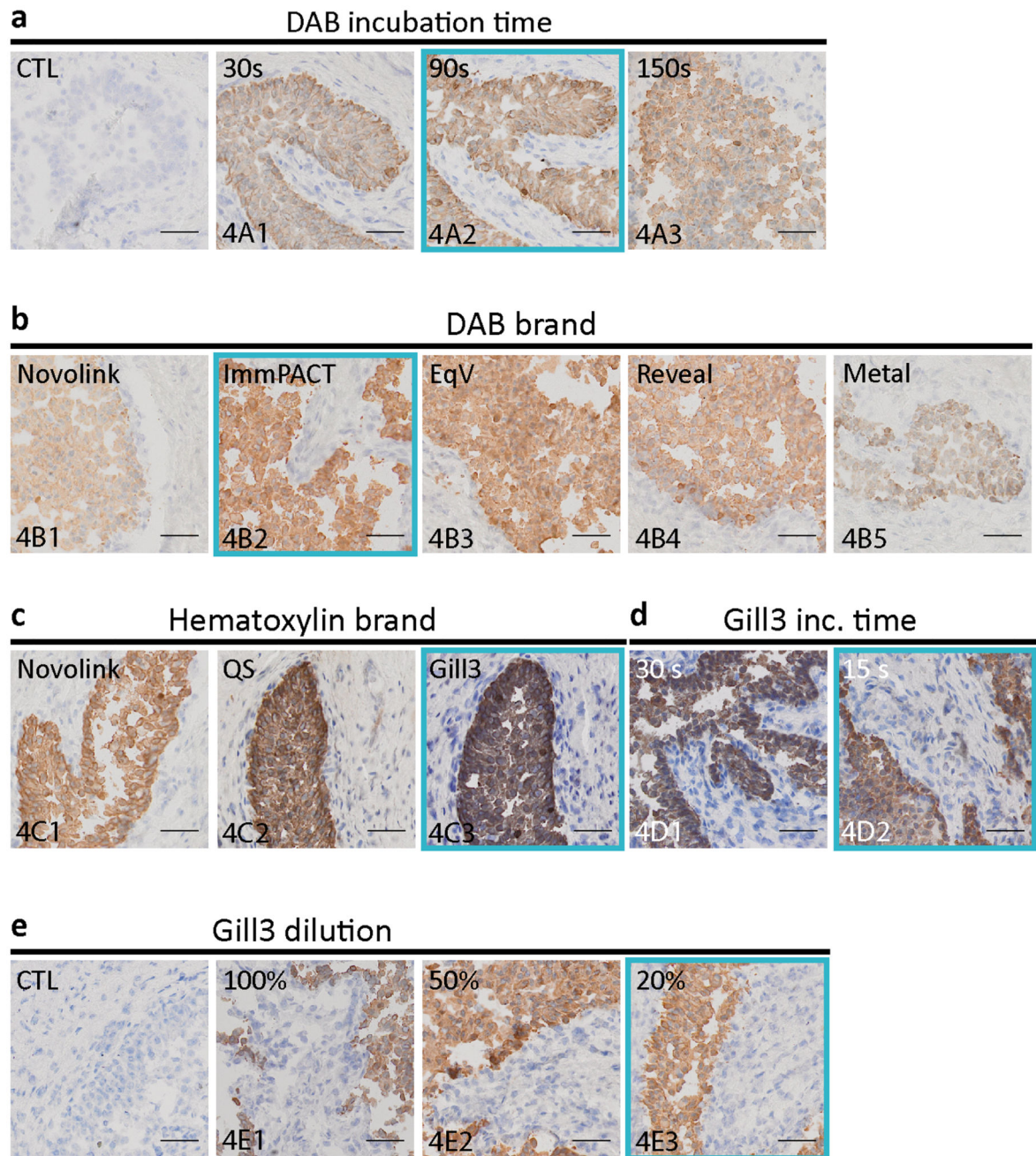


Fig. 4. Optimization of the second part of the MTP staining protocol of Table 1 on ureteral biopsy sections.

(a) Optimization of the incubation time of DAB obtained from the Novolink kit. Increasing the DAB incubation time between 30 s and 90 s increases the intensity of the signal. However, no difference is perceived between 90 s and 150 s, indicating that incubation longer than 90 s is not necessary. (b) DAB reagents from 5 manufacturers were compared under the same experimental conditions. ImmPACT was selected as giving the best staining quality. (c) Three hematoxylin suppliers were compared, giving as most suitable choice

hematoxylin obtained from Gill3. **(d)** The optimized hematoxylin incubation time was chosen as 15 s. **(e)** Finally, we diluted the hematoxylin solution to 20% of its original concentration using DIW, resulting in lesser viscosity and eosin application without compromising the staining. (Scale bars: 50 μm ; bottom-left code: identifier of the sample in Table S1).

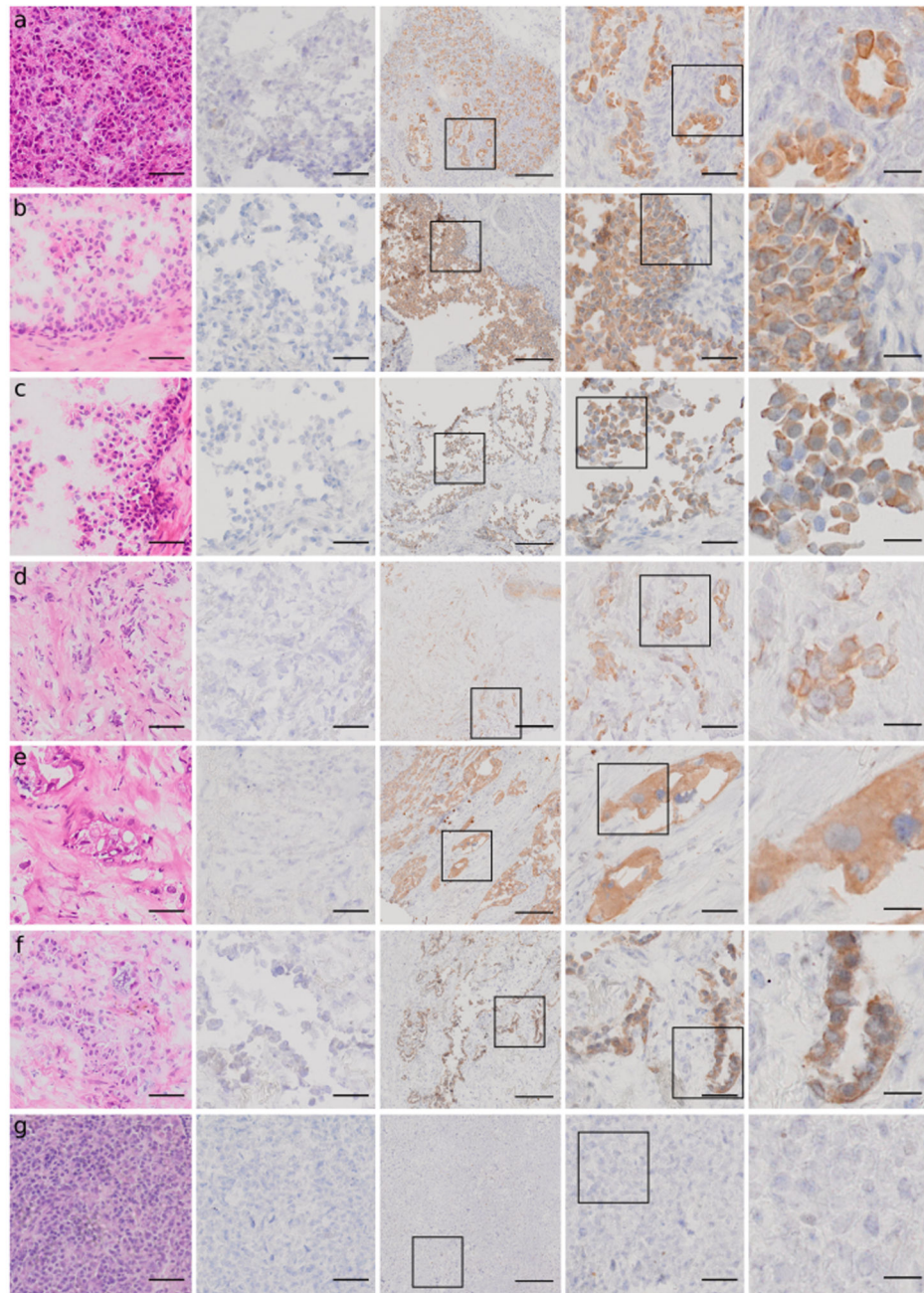


Fig. 5. Results of the optimized MTP staining protocol for different tissue types for CK in IHC (less than 12 minutes) and H&E (2:30 minutes).

Optimized H&E staining (first column), CTL staining (negative control, second column), and CK staining at 3 magnifications: scale bar 200 μm (third column), scale bar 50 μm (fourth column) and 20 μm (fifth column) performed on the following samples: pancreas (a), ureter (b), prostate (c), breast carcinoma (d), pancreas adenocarcinoma (e), lung carcinoma (NSCLC) (f), Hodgkin lymphoma (g). The H&E stainings were performed on the MTP in 2:30 minutes. CK staining showed specificity to epithelial cells on non-cancerous tissues and on carcinomas of different origin. At the same time, no false-positive staining was

observed on the lymphoma case. Similarly, the negative controls, where the protocols were run without primary anti-CK Abs, showed only nuclear counterstaining, as expected. (Scale bars: 50 μm for columns 1, 2 and 4; 200 μm for column 3 and 20 μm for column 5).

Table 1**Staining protocols.**

Details of the complete protocol for (i) manual staining, (ii) initial MTP protocol, which was based on previous experiments on formalin-fixed paraffin-embedded samples^{20,21} and (iii) optimized MTP protocol realized in this study. Washing steps, performed in-between the described steps, are not explicitly mentioned. The overall washing time is shown at the end of the table.

| Step number | Group | Step | (i) Manual protocol Time (min) | | (ii) Initial MTP protocol Time (min) | | (iii) Optimized MTP protocol Time (min) | |
|--------------------------------|------------------|--------------------|--------------------------------------|----------|--|----------|---|----------|
| 1 | PRE – STAINING | Sectioning | 0.0 | Off chip | 0.0 | Off chip | 0.0 | Off chip |
| 2 | | First drying | 15.0 | | 15.0 | | 2.0 | |
| 3 | | Fixation | 10.0 | | 10.0 | | 3.0 | |
| 4 | | Second drying | 15.0 | | 15.0 | | 2.0 | |
| 5 | | Re-hydration | 15.0 | | 15.0 | | 1.0 | |
| PRE-STAINING subtotal | | | 55.0 | | 55.0 | | 8.0 | |
| 6 | STAINING PART I | Peroxidase block | 5.0 | | 2.0 | On chip | 0.0 | |
| 7 | | Protein block | 5.0 | | 2.0 | | 0.0 | |
| 8 | | Primary antibody | 30.0 | | 4.0 | | 2.0 | |
| 9 | | Post primary | 30.0 | | 4.0 | | 0.0 | |
| 10 | | Secondary antibody | 30.0 | | 4.0 | | 4.0 | |
| 11 | STAINING PART II | DAB | 5.0 | | 2.5 | Off chip | 1.5 | |
| 12 | | Counterstaining | 5.0 | | 4.0 | | 0.3 | |
| STAINING subtotal (no washing) | | | 110.0 | | 22.5 | | 7.8 | |
| Washing | | | 105.0 | | 5.8 | | 3.3 | |
| STAINING subtotal | | | 215.0 | | 28.3 | | 11.1 | |
| TOTAL | | | 270.0 | | 83.3 | | 19.1 | |